

Transcranial magnetic stimulation modulates the brain's intrinsic activity in a frequency-dependent manner

Mark C. Eldaief^{a,b,1}, Mark A. Halko^a, Randy L. Buckner^{c,d,e,f,g}, and Alvaro Pascual-Leone^{a,b}

^aBerenson-Allen Center for Noninvasive Brain Stimulation, and ^bDivision of Cognitive Neurology, Department of Neurology, Beth Israel Deaconess Medical Center, Harvard Medical School, Boston, MA 02215; ^cDepartment of Psychology and ^dCenter for Brain Science, Harvard University, Cambridge, MA 02138; ^eAthinoula A. Martinos Center for Biomedical Imaging, Massachusetts General Hospital, Charlestown, MA 02129; ^fDepartment of Psychiatry, Massachusetts General Hospital/Harvard Medical School, Boston, MA 02215; and ^gHoward Hughes Medical Institute, Cambridge, MA 02138

Edited by Marcus E. Raichle, Washington University in St. Louis, St. Louis, MO, and approved November 15, 2011 (received for review August 10, 2011)

Intrinsic activity in the brain is organized into networks. Although constrained by their anatomical connections, functional correlations between nodes of these networks reorganize dynamically. Dynamic organization implies that couplings between network nodes can be reconfigured to support processing demands. To explore such reconfigurations, we combined repetitive transcranial magnetic stimulation (rTMS) and functional connectivity MRI (fcMRI) to modulate cortical activity in one node of the default network, and assessed the effect of this upon functional correlations throughout the network. Two different frequencies of rTMS to the same default network node (the left posterior inferior parietal lobule, lpIPL) induced two topographically distinct changes in functional connectivity. High-frequency rTMS to lpIPL decreased functional correlations between cortical default network nodes, but not between these nodes and the hippocampal formation. In contrast, low frequency rTMS to lpIPL did not alter connectivity between cortical default network nodes, but increased functional correlations between lpIPL and the hippocampal formation. These results suggest that the default network is composed of (at least) two subsystems. More broadly, the finding that two rTMS stimulation regimens to the same default network node have distinct effects reveals that this node is embedded within a network that possesses multiple, functionally distinct relationships among its distributed partners.

network dynamics | resting-state functional MRI | hippocampus | medial prefrontal cortex

Intrinsic activity in the brain is organized into networks (1). Functional connectivity MRI (fcMRI) analyses have used spontaneous low-frequency oscillations in the blood oxygenation level-dependent (BOLD) signal to show that nodes within these networks are functionally correlated with one another (2; for reviews see refs. 3 and 4). Although intrinsic brain networks are constrained by an anatomical skeleton, the strength of functional connectivity between network regions is dynamic (1, 5, 6). Consequently, there is growing interest in characterizing how networks of brain regions dynamically change their couplings to form multiple possible functional configurations.

Transcranial magnetic stimulation (TMS) affords an opportunity to explore such alternative configurations by modulating intrinsic activity networks. Repetitive TMS (rTMS) alters local cortical activation in a temporally sustained fashion (7, 8), and permits the targeting of predetermined cortical regions. rTMS is particularly well suited to study changes across cortical networks (9, 10). Local stimulation to an accessible network node can propagate, via transsynaptic means, to distal but interconnected nodes with high spatial specificity (11, 12). This approach allows for causality to be inferred between the applied stimulation and the observed changes in network connectivity.

The default network is comprised of a set of distributed brain regions, including the medial prefrontal cortex (mPFC), the posterior cingulate cortex/ventral precuneus (pCC), the posterior

inferior parietal lobule (pIPL), and the hippocampal formation (HF) (13–16). As several fcMRI studies have detailed the strength of functional connectivity between these regions (17–19), we endeavored to study the effects of rTMS modulation upon intrinsic connectivity in the default network.

We used an “off-line” fcMRI-rTMS paradigm in which functional connectivity within the default network was measured with fcMRI both immediately before and immediately after rTMS (20). Using a within-subject design, a group of healthy participants underwent two separate sessions of rTMS in counter-balanced order, receiving the same number of rTMS stimuli, over a similar time frame, to the same cortical node of the default network [left pIPL (lpIPL)], but applied in trains of two different frequencies. The use of MRI-guided, neuronavigated rTMS enabled targeting of the same cortical region across subjects and stimulation sessions. Changes in interregional functional connectivity as a result of the rTMS intervention were measured within each subject. We hypothesized that manipulating activity in a targeted default network node with high- (20 Hz) and low- (1 Hz) frequency rTMS would have opposing effects upon network connectivity. We based this expectation on human and animal studies demonstrating that low-frequency rTMS renders a suppressive effect upon cortical excitability in the targeted cortical region, whereas high-frequency rTMS exerts a facilitatory effect on the cortical region being stimulated (21–23). Moreover, the bidirectional effects of high- and low-frequency stimulation upon local cortical excitability have been shown to translate to bidirectional changes in interregional connectivity. For example, Rounis et al. used effective connectivity to show that high- and low-frequency rTMS to M1 induced opposing effects on task-related motor network connectivity (24). We also predicted that a given rTMS frequency would induce comparable changes in functional connectivity across the entire network, independently of the anatomical region-to-region correlation being assessed. For example, if a given frequency were to decrease functional connectivity between lpIPL and mPFC, it should also decrease connectivity between lpIPL and left HF (lHF).

Results

Participants completed the experimental design depicted in Fig. 1. First, each participant underwent a baseline resting-state fMRI (rs-fMRI). An fcMRI analysis was performed on this baseline functional data to delineate each participant's default

Author contributions: M.C.E., M.A.H., R.L.B., and A.P.-L. designed research; M.C.E. and M.A.H. performed research; R.L.B. contributed analytic tools; M.A.H. analyzed data; and M.C.E., M.A.H., R.L.B., and A.P.-L. wrote the paper.

Conflict of interest statement: A.P.-L. serves on the scientific advisory board for Nexstim, Neuronix, Starlab, and Neosync, and is an inventor of several issued and applied patents for the combination of transcranial magnetic stimulation with EEG and neuroimaging.

This article is a PNAS Direct Submission.

¹To whom correspondence should be addressed. E-mail: meldaief@bidmc.harvard.edu.

This article contains supporting information online at www.pnas.org/lookup/suppl/doi:10.1073/pnas.1113103109/-DCSupplemental.

network, and to anatomically localize the lpIPL node. Participants then returned for two subsequent stimulation sessions (on separate days, at least 1 wk apart): one in which they received 1-Hz rTMS to lpIPL, and another in which they received 20-Hz rTMS to lpIPL. The order of the 1-Hz and 20-Hz stimulation sessions was counterbalanced across participants. During rTMS, a stereotactic optical tracking neuronavigation system, loaded with the participant's baseline functional connectivity data, was used to target the predetermined lpIPL node and to target this same cortical region during both stimulation sessions. Participants completed two rs-fMRI scans: one immediately before, and another immediately following, rTMS stimulation to lpIPL. To assess the effect of rTMS upon functional connectivity in the default network, we performed a seed-based fcMRI analysis of functional MRI data acquired before and after stimulation in each participant. This analysis was accomplished by placing seeds in six default network regions of interest: lpIPL (the stimulation site), right pIPL (rpIPL), pCC, mPFC, IHF and right HF (rHF). Critically, the six regions used to assess changes in functional connectivity as a result of rTMS were defined a priori on the basis of each participant's individualized baseline fMRI resting-state data. The mean Montreal Neurological Institute (MNI) coordinates of the six regions across participants are displayed in Table S1. Changes in region-to-region correlation strengths (i.e., post-rTMS minus pre-rTMS) were then computed between these six regions, and this constituted the main outcome of interest.

To test our predictions about the effects of the two frequencies of rTMS upon functional connectivity, we first examined functional connectivity changes as a result of rTMS between the stimulation site (lpIPL) and the other five default network regions, yielding the following region pairs: lpIPL-rpIPL, lpIPL-mPFC, lpIPL-pCC, lpIPL-IHF, and lpIPL-rHF. We expected a significant main effect of frequency upon functional connectivity, but no main effect of region pair. We did not predict an interaction between frequency and region pair because we hypothesized that the changes in functional connectivity induced by 1 Hz and 20 Hz would occur in opposing directions. An independent-measures ANOVA assessing the difference in mean change in functional connectivity involving these five region pairs (REGION) and across both frequencies of stimulation (FREQ) revealed a significant effect of REGION [$F(4,160) = 4.35$, $P < 0.05$] and a significant effect of FREQ [$F(1,160) = 24.40$,

$P < 0.05$]. No interaction was found between REGION and FREQ [$F(5,160) = 0.32$, $P = 0.87$]. Fig. 2 displays the observed mean changes in functional connectivity among region pairs involving the lpIPL stimulation site. Consistent with our initial hypotheses, the two frequencies induced opposite effects (1 Hz elicited positive changes and 20 Hz elicited negative changes). Contrary to our initial assumption, the two frequencies induced topographically distinct changes in functional connectivity. rTMS induced a positive change in selected region pairs with one frequency, a negative change in other region pairs with another frequency, and no change otherwise.

Paired *t* tests revealed that 20-Hz stimulation resulted in significant decreases in functional connectivity between lpIPL-mPFC [$t(16) = -4.61$; $P < 0.05$ Bonferroni-corrected] and lpIPL-rpIPL [$t(16) = -3.16$; $P < 0.05$ Bonferroni-corrected]. Correlations were also reduced between lpIPL-pCC as a result of 20-Hz stimulation, but this did not survive multiple comparison corrections: lpIPL-pCC [$t(16) = -2.80$; $P < 0.05$, uncorrected; $P = 0.06$ Bonferroni-corrected]. Correlations between lpIPL and rHF and IHF did not show significant changes as a result of 20-Hz stimulation: lpIPL-IHF [$t(16) = -0.371$; $P > 0.05$, uncorrected]; lpIPL-rHF [$t(16) = -0.775$; $P > 0.05$, uncorrected]. The 1-Hz stimulation resulted in significant increases in functional connectivity between lpIPL-IHF [$t(16) = 4.17$; $P < 0.05$ Bonferroni-corrected]. None of the other four region pairs showed significant changes to 1-Hz stimulation (all $P > 0.05$, uncorrected).

Qualitatively, these topographically distinct effects can be appreciated by examining functional connectivity maps derived from the lpIPL seed region (i.e., from the stimulation site) before and after rTMS (Fig. 3). Visually similar maps that included distributed regions of the default network were derived before and following rTMS to lpIPL (Fig. 3 *A* and *B* for high- and Fig. 3 *D* and *E* for low-frequency rTMS). Voxel-wise paired *t* test maps that directly examined the effects of rTMS indicated significant changes in functional correlations that were consistent with the region of interest analysis. Specifically, following 20-Hz rTMS, functional correlations decreased between lpIPL and pCC, and between lpIPL and mPFC, but no correlation changes were appreciated between lpIPL and HF (Fig. 3*C*). Following 1-Hz stimulation, functional connectivity increased between lpIPL and HF, but not between lpIPL and either pCC, mPFC, or rpIPL (Fig. 3*F*).

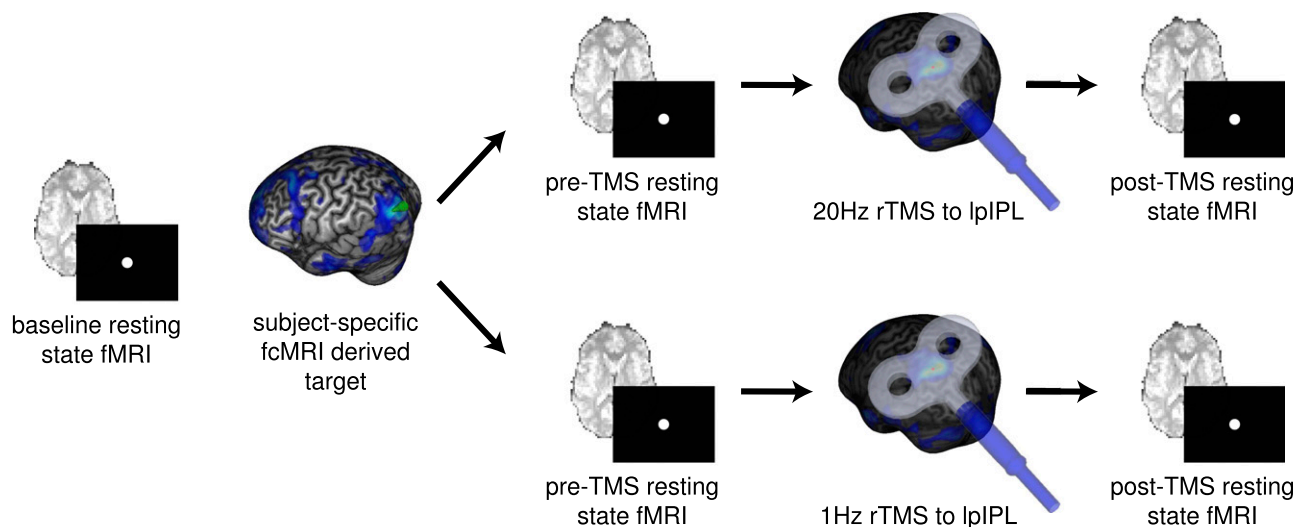


Fig. 1. Experimental design. Each participant first underwent a baseline resting-state fcMRI scanning session to allow for the creation of individualized functional connectivity maps localizing the lpIPL node of their default network. This node served as the future target for two subsequent rTMS stimulation sessions (on separate days): one in which they received 1-Hz rTMS to lpIPL, and another in which they received 20-Hz rTMS to lpIPL. Consistent targeting of lpIPL across sessions was achieved by using a frameless stereotactic neuronavigation system. During each of the two stimulation sessions, subjects completed two fcMRI scans: one immediately before, and another immediately following rTMS.

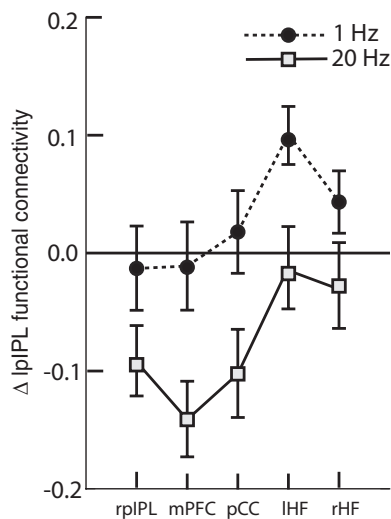


Fig. 2. Changes in functional connectivity in the default network as a result of the two frequencies of rTMS. Changes in functional connectivity are shown between the site of rTMS stimulation (lpIPL) and the five other a priori determined default network regions following 20-Hz (solid line) and 1-Hz (dashed line) stimulation across all participants. The y axis represents changes in z-transformed region-to-region correlation strength as a result of rTMS to lpIPL. The regions of interest used for the functional connectivity analysis are shown on the x axis. Error bars represent one SEM. Twenty-hertz and 1-Hz rTMS induced opposing effects upon default network functional connectivity, and did so in a topographically distinct pattern.

We then examined the frequency-dependent effects of rTMS across default network regions that were not directly stimulated (again with the locations of these derived from participant's baseline fcMRI data). We computed difference measures resulting from rTMS for the following ten region pairs: rpIPL-pCC, rpIPL-mPFC, rpIPL-IHF, rpIPL-rHF, pCC-mPFC, pCC-IHF, pCC-rHF, mPFC-rHF, mPFC-IHF, and IHF-rHF. An independent-measures ANOVA demonstrated a significant effect of FREQ [$F(1,320) = 6.33, P < 0.05$], but no significant effect of REGION [$F(9,320) = 1.39, P > 0.05$], nor was there an interaction between REGION and FREQ [$F(9,320) = 0.63, P > 0.05$]. Paired *t* tests revealed that 20-Hz stimulation decreased functional connectivity between rpIPL-mPFC and between

rpIPL-pCC, but these did not survive multiple comparison corrections: rpIPL-mPFC [$t(16) = -2.98; P < 0.05$, uncorrected; $P = 0.08$ Bonferroni-corrected] and rpIPL-pCC [$t(16) = -2.55; P < 0.05$, uncorrected; $P = 0.21$ Bonferroni-corrected]. All other region pairs did not show significant changes as a result of 20-Hz stimulation (all $P > 0.05$, uncorrected). The 1-Hz stimulation resulted in increased functional connectivity between rpIPL and IHF, but this did not survive multiple comparison corrections [$t(16) = 3.23; P < 0.05$, uncorrected; $P = 0.05$ Bonferroni-corrected]. All other region pairs did not show significant changes in response to 1-Hz stimulation (all $P > 0.05$, uncorrected). Fig. 4 displays a schematic of functional connectivity changes across the entire default network as a result of 1-Hz and 20-Hz rTMS.

It could be argued that the observed changes in functional connectivity between pre- and post-rTMS scanning sessions were not the result of the rTMS stimulation, but were rather due to the inherent variability of network functional connectivity between two rs-fMRI acquisitions separated in time. To examine this possibility, we compared changes in functional connectivity between participants' pre-rTMS scans. There were no significant changes across any of the 15 default network region pairs (the five associated with lpIPL and the 10 associated with regions not directly stimulated) across participants' pre-1-Hz and pre-20-Hz scans (all $P > 0.05$, uncorrected). We also observed significant intersubject variability across pre-rTMS sessions, and between post- and pre-rTMS scans within sessions in which no significant changes in functional connectivity occurred. The intersubject variability is represented by the example in Fig. 5. The majority of participants exhibited decreases in functional connectivity between lpIPL and mPFC following 20 Hz, but there was considerable intersubject variability in the correlation changes between lpIPL and mPFC following 1 Hz, and across their pre-1-Hz and their pre-20-Hz scans.

To assess the possibility that changes in functional connectivity were not reflective of the dynamic properties of the default network, per se, but were the result of nonspecific effects of the stimulation throughout the brain, we constructed three extra-network control regions: primary sensorimotor cortex (SM1), primary auditory cortex (A1), and primary visual cortex (V1). V1 was not expected to be affected by the rTMS paradigm applied in the present experiment. SM1 was considered a useful control region because it might have been modulated by the tapping sensation produced by the application of rTMS. Finally, A1 was considered a particularly powerful control region, as our stimulation likely activated it because of the loud clicking noise

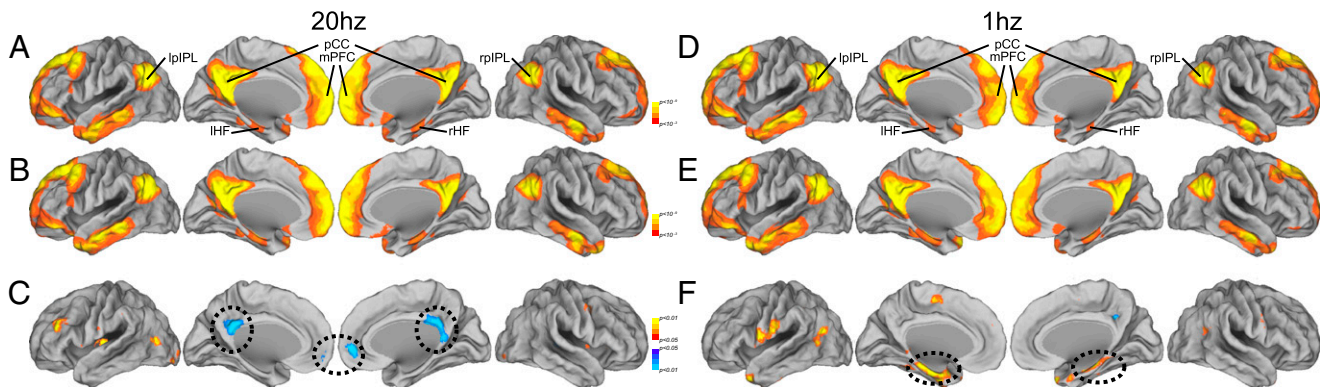


Fig. 3. Functional connectivity maps derived from an lpIPL seed region before and after rTMS. Maps are displayed before (A), after (B), and as the change between before and after (C) 20-Hz rTMS stimulation, and before (D), after (E), and as the change between before and after (F) 1-Hz rTMS stimulation to the lpIPL across all participants. The maps represent uncorrected *P* values at each location for a voxel-wise one-sample *t* test for z-transformed correlation coefficients greater than 0 (A, B, D, and E). For difference measures, the maps represent uncorrected *P* values for a voxel-wise repeated-measures *t* test comparing z-transformed correlation coefficients before stimulation to after stimulation (C and F). Following 20-Hz stimulation, decreases in functional connectivity with respect to lpIPL were observed in pCC and in mPFC, highlighted with black dotted ovals. Following 1-Hz stimulation, increases in functional connectivity were observed between the lpIPL seed and the bilateral hippocampal formation (left and right HF), indicated with black dotted ovals.

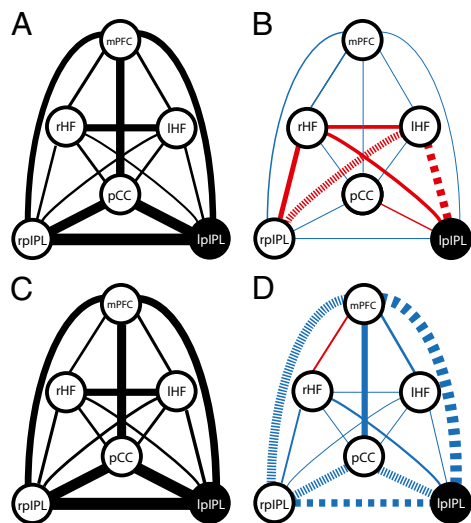


Fig. 4. Schematic representation of functional connectivity changes across multiple regions within the default network. The thickness of the lines connecting default network regions is proportional to the connectivity strength between these regions. Connectivity is displayed before 1-Hz (A) and 20-Hz (C) rTMS (Left). (Right) Changes in functional connectivity between default network regions as a result of 1-Hz (B) and 20-Hz (D) rTMS. Scaling of line thickness to changes in correlation strength is different between Right and Left. Decreases in functional connectivity are depicted with blue lines, and increases are depicted in red. Large dashed lines signify significant changes (corrected for multiple comparisons). Small dashed lines signify significant correlation changes not surviving multiple comparisons corrections. These results suggest coupling between regions in the default network is dynamic.

associated with the rTMS discharge. Prior TMS-fMRI paradigms have shown that SM1, and particularly A1, are activated by the administration of TMS (25). We found no significant change when comparing post- minus pre-rTMS interhemispheric functional correlations (e.g., left A1 to right A1) with respect to any of these three control regions. Furthermore, we found no significant changes in functional correlations between right or left SM1, A1, or V1 and any of the six default network regions, neither with respect to high-, nor with respect to low-frequency stimulation (all $P > 0.05$). Fig. S1 contrasts changes in functional connectivity between lpIPL and the remainder of the default network, and between left A1 and the default network following the two rTMS frequencies.

Discussion

We used rTMS to demonstrate that modifying cortical excitability in one node of the default network with two different patterns of stimulation induced two distinct, quantitatively different changes in network functional connectivity. High-frequency stimulation decreased functional connectivity among the mPFC, pCC, and pIPL nodes, whereas low-frequency stimulation increased functional connectivity between lpIPL and lHF. This finding suggests that the default network is composed of (at least) two interacting functional configurations or subsystems: one encompassing mPFC, pCC, and pIPL and another consisting of pIPL and HF. Graph theory and hierarchical clustering analyses have previously been used to suggest the existence of discrete functional default network subsystems, with the medial temporal lobe being functionally segregated (17). In addition, task-based fMRI studies have demonstrated preferential activation of the medial temporal subsystem of the default network under certain conditions (17). Although these approaches are useful, there are advantages to using rTMS to delineate intrinsic network subcomponents. Given the unconstrained nature of intrinsic activity, it can be difficult to draw causality (26). In

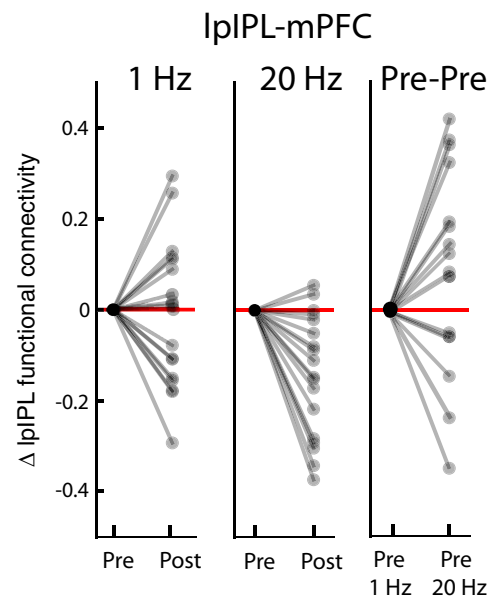


Fig. 5. Changes in functional connectivity with and without intervening rTMS. Plots indicate relative changes (normalized to zero values for pre-rTMS connectivity) for each participant between the stimulation site (lpIPL) and mPFC. The majority of participants showed a decrease in functional connectivity between lpIPL and mPFC following 20-Hz (Center), but no change and significant intersubject variability occurred following 1 Hz (Left) and across their pre-1-Hz and pre-20-Hz rTMS sessions (Right).

addition, task-based experiments may depend on a subject's effort, performance level, or task strategy (27). In contrast, rTMS allows for causality to be inferred between the stimulation and the measured changes in functional connectivity. rTMS also has advantages over statistical modeling of fMRI data, as it is an extrinsic perturbation of functional connectivity, and therefore an empirical test of what configurations the network can assume.

The specific network configurations we observed as a result of rTMS may be accounted for by the anatomical connectivity between lpIPL and its default network counterparts. pIPL has reciprocal anatomical connections with both the pCC and the medial temporal lobe. Tracer studies in the macaque have demonstrated projections between the posterior cingulate (specifically area 23) and area 7a (28) (an area which is at or near the putative homolog of the human pIPL node) (14). Reciprocal projections between 7a and the parahippocampal cortex are also present (29).

Still, there is evidence that intrinsic networks cannot be fully understood on the basis of anatomical connectivity alone. Whereas functional connectivity in the default network partially parallels anatomical connections (14, 30), functional connectivity exists in the absence of monosynaptic anatomical connectivity (6). For example, in the macaque functional correlations are present in the visual system where no anatomical connections exist (31). This finding implies that functional connectivity is also mediated through indirect (possibly polysynaptic) anatomical connections, with functional correlations reflecting a "functional gating" of anatomical pathways (6). Our data serve to further underscore the principle that intrinsic network organization is constrained by, but not dictated by, anatomical connectivity.

Our findings specifically demonstrate that functional connectivity within intrinsic networks is dynamic. Functional couplings within the default network are often conceptualized as being static, with connectivity assessments remaining relatively constant across scanning sessions (32). However, such static depictions may have arisen from the ways in which intrinsic networks are analyzed. fMRI analyses typically compute region-to-region functional connectivity across an entire scanning session, with

the assumption that the strength of these couplings do not change appreciably across the sampled time window (33, 34). Two approaches have recently challenged this framework. First, computational network modeling has emphasized dynamic properties of large scale networks. Honey et al. (35) created a computational network model (based on anatomical data of the macaque neocortex) to identify functional networks between anatomically connected regions in the resting state. Their neural mass model, in which each network region was represented by a chaotic oscillator, revealed that the network recapitulated structural connectivity over long time periods. However, over short time intervals (i.e., seconds), the strength of functional connectivity between network nodes fluctuated in ways that were not predictable based on the network's anatomical organization. Computational models have also illustrated temporally dynamic effects of simulating lesions in discrete nodes or edges of neural networks (36). Second, recent analyses of fMRI data have emphasized novel approaches to uncover temporal changes in functional connectivity over the course of a single scanning session. Chang and Glover (33) performed a wavelet coherence analysis of fMRI data and showed that functional correlations between pCC and other cortical nodes fluctuated in a time-dependent manner. Majeed et al. (34) used a novel algorithm to demonstrate that the spatiotemporal patterns of functional connectivity between two intrinsic activity networks vary over short time scales. These investigations, along with our results, suggest that individual nodes of intrinsic networks may be embedded within dynamic systems.

Further exploration of intrinsic network dynamics using TMS and fMRI would benefit from greater understanding of the physiologic effects of rTMS on the directly targeted brain region. Studies have emphasized interindividual variability in the neuromodulatory effects of rTMS as a function of the rTMS frequency applied (23). Furthermore, as the effects of TMS have been shown to be state-dependent (37), lpIPL may have responded differently to the two frequencies because of disparities in ongoing levels of tonic activation (38). In this light, the pre-rTMS activity could serve to partially determine the degree and direction of cortical excitability changes at pIPL as a way of maintaining a homeostatic level of cortical activation within a physiologically useful range (39). This notion is supported by studies demonstrating that preconditioning cortical excitability with other forms of brain stimulation alters the expected plastic effects of subsequent rTMS (39, 40). Similar arguments can be made regarding the distributed network effects of local stimulation, wherein metaplastic processes may be involved in maintaining network homeostasis.

The effects of rTMS in our study likely had multiple biophysical determinants, such as the existence of bidirectional connections (excitatory or inhibitory) between network nodes or other network properties (e.g., its modularity, its connection density, and the mean path length among its constituent nodes) (41, 42). It is also conceivable that 1 Hz and 20 Hz differentially altered two neuronal subpopulations in lpIPL, which differed with respect to their anatomical connectivity. Finally, it is feasible that rTMS modulated networks functionally correlated (or anticorrelated) to the default network, or that it altered the functional relationships between lpIPL and these networks. For example, in Fig. 3 *C* and *F* there appear to be correlation changes between lpIPL and regions lying outside of the anatomical boundaries of the default network. Such changes may have been mediated by the direct effects of stimulating lpIPL, or through additional modulations in the excitability profiles of neuronal populations adjacent to lpIPL, which share functional connectivity with other intrinsic networks.

Extensions of our present study may assess the behavioral or cognitive consequences of differential modulation of intrinsic functional connectivity. Our participants did not report subjective changes in cognition following differential modulation of functional connectivity by the two rTMS frequencies, and we did not wish to allow a behavioral task to affect functional connec-

tivity independently of the effects of the stimulation. However, future studies may be able to derive correlations between behavioral performance and directed changes in functional connectivity. Similarly, our results may be relevant to the design of therapeutic interventions. Despite the emergence of brain stimulation to treat neuropsychiatric conditions, there remain challenges to understanding the effects of these regimens upon intrinsic networks. For example, deep brain stimulation to the subgenual cingulate has been used in treatment-resistant major depression (43), and high-frequency rTMS to the left dorsolateral PFC is effective in ameliorating this condition (44). In addition, aberrant functional connectivity with the subgenual cingulate has been described in major depression, and has been correlated to disease severity (45). However, whether deep brain stimulation or rTMS inhibit maladaptive intrinsic connectivity configurations like these, and instead promote the formation of more adaptive configurations, is not presently known.

In summary, our study places emphasis on the dynamic relationships between regions of intrinsic brain networks. If, as our data suggest, intrinsic network nodes are embedded within dynamic systems, a thorough understanding of the brain's intrinsic activity must take into account such dynamic properties. For example, it is quite possible that the fluidity of the functional relationships among intrinsic network regions plays a role in supporting different processing demands. The combination of rTMS with fMRI offers a promising methodology to investigate such phenomena in humans.

Methods

Participants. Twenty-five healthy adults (12 female; ages 23–38 y, mean = 26.0, SD = 3.6) without any neuropsychiatric conditions and not on any medications participated in the study. All participants provided written informed consent in accordance with the guidelines of the Committee on Clinical Investigations at the Beth Israel Deaconess Medical Center.

fMRI Acquisition. All MR imaging was conducted at the Center for Biomedical Imaging, at Boston University Medical Center on a 3.0-T whole-body scanner (Phillips, Achieva). MR acquisition parameters are described in detail in *SI Methods*. For each rs-fMRI scan (baseline, pre-rTMS, and post-rTMS), functional data were collected by using an asymmetric spin-echo, echo-planar sequence sensitive to BOLD contrast during three 6-min functional runs.

fMRI/TMS Sessions. All participants first underwent a baseline scanning session. This was done to accrue participants' individualized functional data in order to perform functional connectivity analyses that would delineate the location of their lpIPL node. Specifically, using an fMRI seed voxel-based analysis, three default network regions were seeded: pCC, mPFC, and rpIPL. The locations of these seed regions were based upon established MNI coordinates (46). In each participant, the three resultant connectivity maps yielded a correlation cluster in lpIPL. A target was then placed in the averaged center of the resultant lpIPL correlation cluster (formed from the overlay of the lpIPL clusters derived from the three connectivity maps) on the cortical surface using theBrainsight neuronavigation software (Brainsight, Magstim; Rogue Research).

After their baseline session, participants underwent two fMRI sessions on separate days at least 1 wk apart (similar to their baseline session): one before and one after rTMS (Fig. 1). Immediately following their pre-rTMS MRI session, each participant was taken into an adjacent room for rTMS stimulation of lpIPL. During rTMS, targeting of lpIPL was achieved by loading a participant's baseline functional connectivity data into a frameless stereotactic optical tracking neuronavigation system (Brainsight). This system permitted lpIPL to be reliably stimulated within each session, across sessions, and across participants. The 1-Hz and 20-Hz stimulations were identical with respect to the total number of pulses delivered, the intensity of the stimulation, and were comparable in terms of the total duration of stimulation. Stimulation parameters and procedures are further detailed in *SI Methods*. The post-rTMS scanning protocol was similar to that used for pre-rTMS scanning, with the exception that functional runs preceded structural runs, so that functional data were acquired immediately following rTMS. The average time elapsed from the end of rTMS stimulation to the beginning of the first post-rTMS functional MRI was short (<4 min), and was consistent with the time elapsed between rTMS and fMRI acquisition in a recently published off-line protocol (47). Moreover, the amount of time between rTMS and functional

imaging capture was less than the established duration of the rTMS effects upon cortical excitability, which has been estimated to last from 20 min (21, 22) up to 1 h (48). Time to fMRI acquisition following rTMS was not statistically different [$t(50) = 1.47, P > 0.05$] between 1-Hz and 20-Hz sessions (for 1-Hz sessions mean time to scanning after rTMS = 213 s, SD = 43 s; for 20 Hz sessions mean time to scanning after rTMS = 203 s, SD = 16 s).

fcMRI Data Analysis. MRI data were analyzed using a combination of freely available software packages (e.g., FMRIB Software Library, FSL; Freesurfer; Statistical Parametric Mapping, SPM) and custom, in-house software. fcMRI data analysis is further described in *SI Methods*. After preprocessing, region-to-region correlation strengths, the main outcome measure of interest, were calculated with volumetric seed-based functional connectivity analyses. Correlation maps were produced by extracting the BOLD time course from a “seed” region in the brain, and then computing the correlation coefficient between that time course and the time course from all other brain voxels (2, 3, 18, 31, 46). To assess the effect of rTMS upon functional connectivity in the default network, we performed the same seed-based fcMRI analysis of functional MRI data acquired before and after rTMS stimulation in each participant. The following six default network seed regions were used for the analysis: left and right pPL, pCC, mPFC, and left and right HF. The

regions used to assess changes in functional connectivity as a result of rTMS were defined a priori on the basis of each subject’s individualized baseline fcMRI data. Functional connectivity between two given network regions was measured by the Pearson’s correlation coefficient (r). A Fisher’s r -to- z conversion transformed r values to corresponding values in the z distribution for all subsequent statistical analyses. To measure the region-to-region correlation changes as a result of rTMS (i.e., the difference between post-rTMS and pre-rTMS z values), a paired t test was performed to compare changes in z scores before and after stimulation.

ACKNOWLEDGMENTS. We thank Andrew Ellison and the Center for Biomedical Imaging at Boston University, Cleofé Peña Gómez for assistance with data processing, and Michael D. Fox for useful discussions. Work on this study was supported in part by the Berenson-Allen Foundation, the Harvard Clinical and Translational Science Center (Harvard Catalyst; NCCR-NIH UL1 RR025758), and the Klarman Foundation (to A.P.-L.). M.C.E. was supported by the Mind, Brain, and Behavior Interfaculty Initiative at Harvard University and the Clinical Investigators Training Program of the Beth Israel Deaconess Medical Center and the Harvard-Massachusetts Institute of Technology Division of Health Sciences and Technology.

- Raichle ME (2011) The restless brain. *Brain Connectivity* 1:3–12.
- Biswal B, Yetkin FZ, Haughton VM, Hyde JS (1995) Functional connectivity in the motor cortex of resting human brain using echo-planar MRI. *Magn Reson Med* 34: 537–541.
- Van Dijk KR, et al. (2010) Intrinsic functional connectivity as a tool for human connectomics: Theory, properties, and optimization. *J Neurophysiol* 103:297–321.
- Fox MD, Raichle ME (2007) Spontaneous fluctuations in brain activity observed with functional magnetic resonance imaging. *Nat Rev Neurosci* 8:700–711.
- Deco G, Jirsa VK, McIntosh AR (2011) Emerging concepts for the dynamical organization of resting-state activity in the brain. *Nat Rev Neurosci* 12:43–56.
- Deco G, Corbetta M (2011) The dynamical balance of the brain at rest. *Neuroscientist* 17:107–123.
- Allen EA, Pasley BN, Duong T, Freeman RD (2007) Transcranial magnetic stimulation elicits coupled neural and hemodynamic consequences. *Science* 317:1918–1921.
- Mottaghy FM, et al. (2003) Repetitive TMS temporarily alters brain diffusion. *Neurology* 60:1539–1541.
- Hampson M, Hoffman RE (2010) Transcranial magnetic stimulation and connectivity mapping: Tools for studying the neural bases of brain disorders. *Front Syst Neur* 4(40):1–8.
- Paus T (2005) Inferring causality in brain images: A perturbation approach. *Philos Trans R Soc Lond B Biol Sci* 360:1109–1114.
- Ruff CC, et al. (2008) Distinct causal influences of parietal versus frontal areas on human visual cortex: Evidence from concurrent TMS-fMRI. *Cereb Cortex* 18:817–827.
- Bestmann S, Baudewig J, Siebner HR, Rothwell JC, Frahm J (2005) BOLD MRI responses to repetitive TMS over human dorsal premotor cortex. *Neuroimage* 28:22–29.
- Laird AR, et al. (2009) Investigating the functional heterogeneity of the default mode network using coordinate-based meta-analytic modeling. *J Neurosci* 29:14496–14505.
- Buckner RL, Andrews-Hanna JR, Schacter DL (2008) The brain’s default network: Anatomy, function, and relevance to disease. *Ann N Y Acad Sci* 1124:1–38.
- Gusnard DA, Raichle ME (2001) Searching for a baseline: Functional imaging and the resting human brain. *Nat Rev Neurosci* 2:685–694.
- Shulman GL, et al. (1997) Common blood flow changes across visual tasks: II: Decreases in cerebral cortex. *J Cogn Neurosci* 9:648–663.
- Andrews-Hanna JR, Reidler JS, Sepulcre J, Poulin R, Buckner RL (2010) Functional-anatomic fractionation of the brain’s default network. *Neuron* 65:550–562.
- Fox MD, et al. (2005) The human brain is intrinsically organized into dynamic, anticorrelated functional networks. *Proc Natl Acad Sci USA* 102:9673–9678.
- Greicius MD, Krasnow B, Reiss AL, Menon V (2003) Functional connectivity in the resting brain: A network analysis of the default mode hypothesis. *Proc Natl Acad Sci USA* 100:253–258.
- Halko MA, Eldaief MC, Horvath JC, Pascual-Leone A (2010) Combining transcranial magnetic stimulation and fMRI to examine the default mode network. *J Vis Exp pii: 2271, 10.3791/2271*.
- Valero-Cabré A, Payne BR, Pascual-Leone A (2007) Opposite impact on 14C-2-deoxyglucose brain metabolism following patterns of high and low frequency repetitive transcranial magnetic stimulation in the posterior parietal cortex. *Exp Brain Res* 176: 603–615.
- Speer AM, et al. (2000) Opposite effects of high and low frequency rTMS on regional brain activity in depressed patients. *Biol Psychiatry* 48:1133–1141.
- Maeda F, Keenan JP, Tormos JM, Topka H, Pascual-Leone A (2000) Interindividual variability of the modulatory effects of repetitive transcranial magnetic stimulation on cortical excitability. *Exp Brain Res* 133:425–430.
- Rounis E, et al. (2005) Frequency specific changes in regional cerebral blood flow and motor system connectivity following rTMS to the primary motor cortex. *Neuroimage* 26:164–176.
- Hanakawa T, et al. (2009) Stimulus-response profile during single-pulse transcranial magnetic stimulation to the primary motor cortex. *Cereb Cortex* 19:2605–2615.
- Morcom AM, Fletcher PC (2007) Does the brain have a baseline? Why we should be resisting a rest. *Neuroimage* 37:1073–1082.
- Fox MD, Greicius M (2010) Clinical applications of resting state functional connectivity. *Front Syst Neurosci* 4:1–13.
- Kobayashi Y, Amaral DG (2007) Macaque monkey retrosplenial cortex: III. Cortical efferents. *J Comp Neurol* 502:810–833.
- Suzuki WA, Amaral DG (1994) Perirhinal and parahippocampal cortices of the macaque monkey: Cortical afferents. *J Comp Neurol* 350:497–533.
- Greicius MD, Supekar K, Menon V, Dougherty RF (2009) Resting-state functional connectivity reflects structural connectivity in the default mode network. *Cereb Cortex* 19:72–78.
- Vincent JL, et al. (2006) Coherent spontaneous activity identifies a hippocampal-parietal memory network. *J Neurophysiol* 96:3517–3531.
- Shehzad Z, et al. (2009) The resting brain: Unconstrained yet reliable. *Cereb Cortex* 19: 2209–2229.
- Chang C, Glover GH (2010) Time-frequency dynamics of resting-state brain connectivity measured with fMRI. *Neuroimage* 50:81–98.
- Majeed W, et al. (2011) Spatiotemporal dynamics of low frequency BOLD fluctuations in rats and humans. *Neuroimage* 54:1140–1150.
- Honey CJ, Kötter R, Breakspear M, Sporns O (2007) Network structure of cerebral cortex shapes functional connectivity on multiple time scales. *Proc Natl Acad Sci USA* 104:10240–10245.
- Honey CJ, Sporns O (2008) Dynamical consequences of lesions in cortical networks. *Hum Brain Mapp* 29:802–809.
- Silvanto J, Muggleton N, Walsh V (2008) State-dependency in brain stimulation studies of perception and cognition. *Trends Cogn Sci* 12:447–454.
- Ruzzoli M, et al. (2011) The effect of TMS on visual motion sensitivity: An increase in neural noise or a decrease in signal strength? *J Neurophysiol* 106:138–143.
- Lang N, et al. (2004) Preconditioning with transcranial direct current stimulation sensitizes the motor cortex to rapid-rate transcranial magnetic stimulation and controls the direction of after-effects. *Biol Psychiatry* 56:634–639.
- Siebner HR, et al. (2004) Preconditioning of low-frequency repetitive transcranial magnetic stimulation with transcranial direct current stimulation: Evidence for homeostatic plasticity in the human motor cortex. *J Neurosci* 24:3379–3385.
- Achard S, Salvador R, Whitcher B, Suckling J, Bullmore E (2006) A resilient, low-frequency, small-world human brain functional network with highly connected association cortical hubs. *J Neurosci* 26:63–72.
- Bullmore E, Sporns O (2009) Complex brain networks: Graph theoretical analysis of structural and functional systems. *Nat Rev Neurosci* 10:186–198.
- Kennedy SH, et al. (2011) Deep brain stimulation for treatment-resistant depression: Follow-up after 3 to 6 years. *Am J Psychiatry* 168:502–510.
- O’Reardon JP, et al. (2007) Efficacy and safety of transcranial magnetic stimulation in the acute treatment of major depression: A multisite randomized controlled trial. *Biol Psychiatry* 62:1208–1216.
- Greicius MD, et al. (2007) Resting-state functional connectivity in major depression: Abnormally increased contributions from subgenual cingulate cortex and thalamus. *Biol Psychiatry* 62:429–437.
- Vincent JL, Kahn I, Snyder AZ, Raichle ME, Buckner RL (2008) Evidence for a frontoparietal control system revealed by intrinsic functional connectivity. *J Neurophysiol* 100:3328–3342.
- Andoh J, Paus T (2011) Combining functional neuroimaging with off-line brain stimulation: Modulation of task-related activity in language areas. *J Cogn Neurosci* 23:349–361.
- Siebner HR, et al. (2003) Patients with focal arm dystonia have increased sensitivity to slow-frequency repetitive TMS of the dorsal premotor cortex. *Brain* 126:2710–2725.